

## Pion interferometry of quark-gluon plasma

Scott Pratt

*School of Physics and Astronomy, University of Minnesota, Minneapolis, Minnesota 55455*

(Received 24 July 1985)

Pion interferometry is discussed as a tool for viewing ultrarelativistic heavy-ion collisions. Several dynamical scenarios are considered for the phase transition into quark-gluon plasma. Experimental signatures for a first-order phase transition are predicted for collisions where the produced matter has no initial collective motion. Recommendations for future experiments are made.

### I. INTRODUCTION

A transition into a phase of matter where color is deconfined has been predicted for temperatures around 200 MeV. At these temperatures the hadron density is so high that the distinction between the different hadrons is blurred by their overlap. The system is then better described by the quark and gluon degrees of freedom. Ultrarelativistic heavy-ion collisions should produce regions of space of sufficient size and with sufficient energy density that this phase transition could occur and be described with models based on thermal equilibrium.

Yet experiments would not view the matter while it is in the deconfined state. Evidence of the transition must come from studying the particles that are emitted from the region after it has reentered the normal hadronic phase. These particles would largely consist of pions since they are the lightest hadron. Two proposed experimental signatures for a quark-gluon plasma are enhancements in the strange-particle<sup>1</sup> and lepton<sup>2</sup> production. But these are not signatures unless the lifetime of the system is well measured. Pion interferometry should give a good measurement of the lifetime if the experiments can measure the correlation function for different directions of the relative momentum.

The equation of state of the emitting region can only be inferred from experiments when the volume is well understood. Pion correlations give the clearest picture of this volume. Large rapidity correlations may also be a signature for bubbles formed by a phase transition,<sup>3</sup> but this can only be discussed when the size of the bubbles is known.

The phase transition may also make a significant difference in the dynamics of the collision. A first-order phase transition with a large latent heat would mean lower pressures in the deconfined phase and very much lower pressures in the mixed phase regions when compared with the confining phase at the same energy density. The lack of pressure gradients would allow the energy density to remain static for a longer period of time. This could increase the lifetime by an order of magnitude, which can then be measured in the interferometry.

Single particle emission spectra have difficulty showing collective expansion in relativistic heavy-ion collisions.

Collective expansion also manifests itself in the interferometry when the source size is measured for pion pairs with different average momenta. At the very least, pion correlation functions provide another check for any theoretical scenario that might be proposed to accurately describe an ultrarelativistic heavy-ion collision. This tool could be very accurate and decisive due to the tremendous number of pions produced, but only if the experiments are designed to measure the correlation function for all different magnitudes and directions of the pion momenta involved.

We calculate the pion correlation function for two different dynamical scenarios. The first is for stopped matter with spherical symmetry. The matter expands due to the hydrodynamic equations under the constraint of entropy conservation. This scenario may not be the most likely, especially at higher bombardment energies, but it does show most clearly the effects of the phase transition on the dynamics. These effects are clearly manifest in the correlation function. The interferometry is also calculated for the Bjorken scaling solution. Here the interferometry can be used to measure the breakup time of the collision. In this sort of expansion the initial longitudinal expansion dominates the dynamics and it is much harder to see the effects of the phase transition. Pressure is not needed to expand the plasma if it is not initially at rest.

This paper is structured as follows. Section II contains a discussion of how the two-particle correlation function of identical particles as measured in momentum space is used to infer the space-time structure of the emission function. The simple bag-model equation of state is reviewed in Sec. III. Section IV gives the results for a spherically expanding plasma. The interferometry is performed for the case when there is a phase transition and when there is not. The phase transition is shown to affect the expansion very significantly and to give a clear signal in the correlation function. The Bjorken scaling solution is described and evaluated in Sec. V. The phase transition does not have as big an effect with this scenario since the initial conditions are more important than the equation of state in determining the expansion. There are also three appendixes which include discussions of the spherical hydrodynamic code, how the correlation functions are calculated from the results of the code, and the details of shock fronts.

## II. THE POWER OF INTERFEROMETRY

The pion correlation function can be used to measure the size and lifetime of a source.<sup>4</sup> Pions emitted from random sources in a finite volume are correlated in their two-particle momentum distribution in the same way that electrons in a metal are anticorrelated in their spatial distribution due to the fact that they occupy only a finite volume of momentum space. The width of the two-particle correlation in the pion's momentum distribution function is related inversely to the size of the source from which they came. The correlation function is defined:

$$C(\mathbf{p}, \mathbf{q}) = P(\mathbf{p}, \mathbf{q}) / [P(\mathbf{p})P(\mathbf{q})], \quad (2.1)$$

where  $P(\mathbf{p}_1 \cdots \mathbf{p}_n)$  is the probability of observing the pions  $\mathbf{p}_1$  through  $\mathbf{p}_n$  all in the same event. If the probability  $g(\mathbf{p}, \mathbf{x})$  of emitting a pion of momentum  $\mathbf{p}$  from a space-time point  $\mathbf{x}$  is known the correlation function can be predicted:<sup>5</sup>

$$P(\mathbf{p}, \mathbf{q}) = P(\mathbf{p})P(\mathbf{q}) + \int d^4x d^4y g(\mathbf{K}, \mathbf{x}) g(\mathbf{K}, \mathbf{y}) \times \exp[i\mathbf{k} \cdot (\mathbf{x} - \mathbf{y})], \quad (2.2)$$

$$P(\mathbf{p}) = \int d^4x g(\mathbf{p}, \mathbf{x}),$$

where  $\mathbf{K} = (\mathbf{p} + \mathbf{q})/2$  and  $k^\mu = p^\mu - q^\mu$ . Thus, measuring the pion correlation function gives the Fourier transform of the spatial probability for emitting two pions with identical momentum. Corrections can be made to these formulas for the effects of final-state Coulomb interactions, coherence effects due to the source not being completely incoherent, and resonance decays.<sup>6</sup> The interference term in Eq. (2.2) depends on the spatial distribution of pions with the same momentum after they have been emitted. Since  $\mathbf{k} \cdot (\mathbf{x} - \mathbf{y})$  is a Lorentz invariant the argument of the exponential can be boosted independently to a frame where the pions have zero total momentum. In this frame  $k_0 = 0$  and the argument can be written as the product of a vector  $\mathbf{K}^*$  with the separation of the pions after they have been emitted:

$$\begin{aligned} \mathbf{k} \cdot (\mathbf{x} - \mathbf{y}) &= \mathbf{k}^* \cdot [\mathbf{v}_K(x^0 - y^0) - (\mathbf{x} - \mathbf{y})], \\ k_{\text{perp}}^* &= k_{\text{perp}}, \\ k_{\text{parallel}}^* &= \gamma_K^2 k_{\text{parallel}} - \gamma_K^2 k_0 v_K, \end{aligned} \quad (2.3)$$

where  $\mathbf{v}_K$  is the velocity of a pion of momentum  $\mathbf{K}$  and  $\gamma_K = (1 - v_K^2)^{-1/2}$ . The subscripts "parallel" and "perp" refer to the direction of  $\mathbf{K}$ . Since the interference term depends only on the probability of emitting pions with the same momentum, and since the argument in the exponential depends only on the relative positions of the pions with the same momentum after emission, the correlation function measures the final spatial distribution of all those pions emitted with exactly the same momentum. One cannot distinguish between cases where the source was large along the direction of the total momentum or whether the lifetime was long which allowed the pions time to separate in their final state. If a symmetry is expected the lifetime can be inferred by measuring the correlation function both perpendicular and parallel to the total momentum of the pair. A long-lived source does not

separate two identically moving pions in the direction perpendicular to their velocity. Measuring pion pairs with higher total momentum is better for showing this effect, since the pions can separate further along the direction of their momentum during a given lifetime when they are moving faster.

Particles with the same velocity are more likely to have come from that part of the source moving in the direction of the pion pair. If there is collective radial expansion slow pions have a greater part of the source from which they can be emitted than do fast pions.<sup>5</sup> Hence, collective expansion leads to smaller effective source sizes for pion pairs with higher total momentum. A long lifetime leads to larger effective source sizes for pion pairs with higher total momentum. However, the effect of the lifetime disappears unless the correlation function is measured for relative momentum in the same direction as the total momentum. Thus there is truly a wealth of information about the dynamics of the system to be gathered if the correlation function can be measured for different magnitudes of the total momentum and different directions of the relative momentum.

## III. THE BAG-MODEL EQUATION OF STATE

The simplest equation of state that interpolates between the relativistic pion gas at low temperatures and the noninteracting quark-gluon plasma at high temperature is the bag model. Here we will assume massless particles with no conserved quantum number. (Since we are only considering temperatures above 120 MeV the assumption of massless particles is good to within 5%. The pion gas has only three degrees of freedom due to the three types of pions while the deconfined plasma has 16 Bose degrees of freedom and 24 Fermi degrees of freedom. Here strange particles have been neglected. The energy density of the quark-gluon plasma is also given a bag constant that forces the pion gas to be the thermodynamically favored state at low temperatures. The pressure  $P$  and the energy density  $\rho$  of a gas of massless particles at high temperature with  $N_f$  Fermi degrees of freedom and  $N_b$  Bose degrees of freedom are

$$P = (\pi^2/90)(N_b + 7/8N_f)T^4, \quad (3.1)$$

$$\rho = 3P.$$

The pressure and energy density of the hadronic and quark phases are therefore

$$\begin{aligned} P_h &= (3\pi^2/90)T^4, \\ \rho_h &= (9\pi^2/90)T^4, \\ P_q &= (37\pi^2/90)T^4 - B, \\ \rho_q &= (37\pi^2/30)T^4 + B. \end{aligned} \quad (3.2)$$

The two equations of state are shown in Fig. 1 as a function of the energy density. For any given temperature the system will choose to be in the phase with the higher pressure. Equating the pressures of the two phases yields the critical temperature where the phase transition occurs:

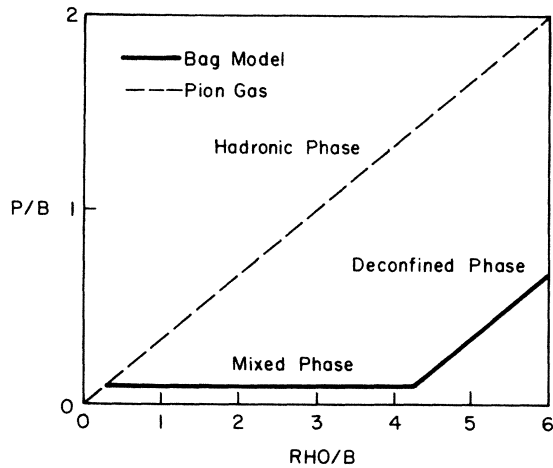


FIG. 1. The first-order phase transition yields a phase of constant pressure. This phase covers a large range of energy densities.

$$\begin{aligned}
 P_q(T_c) &= (37\pi^2/90)T_c^4 - B \\
 &= P_h(T_c) = (3\pi^2/90)T_c^4, \\
 T_c &= (90B/34\pi^2)^{1/4}.
 \end{aligned}
 \tag{3.3}$$

The energy densities of the two phases are different when they are at this critical temperature. The bag model has some support in the fact that a first-order phase transition also shows up in much more complicated analyses such as lattice Monte Carlo analyses.<sup>7</sup> Figure 2 (Ref. 8) shows the discontinuity in energy density as a function of temperature for a gluon gas in QCD. There is still great difficulty in treating the Fermi degrees of freedom effectively. It is surprising how closely the plasma phase resembles an ideal gas.

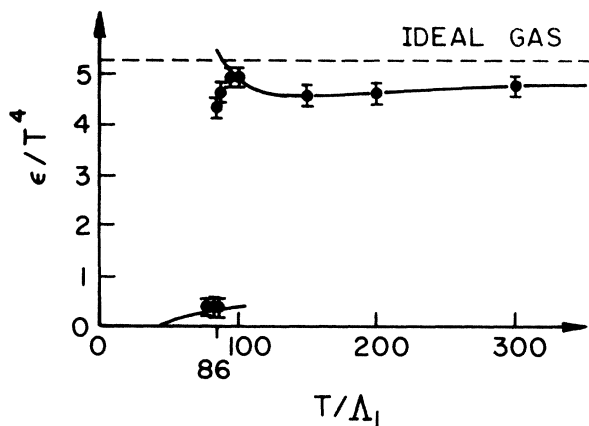


FIG. 2 The energy density from a Monte Carlo simulation of quarkless SU(3) on an  $8^3 \times 3$  lattice shows a discontinuity meaning a first-order phase transition. The low-temperature phase corresponds to massive glueballs while the high-temperature phase corresponds to perturbative plasma. The solid curves are calculated from perturbation theory. The dashed line represents a noninteracting gas of gluons.

There is a range of energy densities between  $\rho_h(T_c)$  and  $\rho_q(T_c)$  where the matter is in a mixed phase. The pressure and temperature are constant throughout this range of energy densities. The fact that the pressure does not change for a range of entropy densities means that the sound velocity is zero in a region of mixed phase. The fluid elements in this region cannot react to adjacent elements until the adjacent elements have a different pressure. This requires a discontinuity in the energy and entropy densities.<sup>9</sup> If a region of space is static and in the mixed phase and it is surrounded by matter in the hadronic phase the matter in the mixed phase cannot expand until a shock wave carrying the discontinuity arrives from the outside. The speed at which the shock wave advances and the properties of the matter just outside the shock front can be found by requiring conservation of energy and momentum across the front while making some assumption about the amount of entropy produced. Shocks are discussed in Appendix C.

When there is a nonzero baryon number the pressure in the mixed phase will depend on the energy density and entropy per baryon. A mixture of two phases at equilibrium will always share the same pressure and the same baryon chemical potential:

$$P_q(\mu, T) = P_h(\mu, T). \tag{3.4}$$

This yields  $\mu(T)$  for any temperature that can support a mixed phase. To solve for an isentrope one must pick a specific ratio of entropy to baryon number. One can now solve for the temperature and chemical potential for any ratio of phase mixtures that give the correct entropy. Defining  $f_q$  and  $f_h$  as the proportion of the baryon number in the quark and hadronic phases ( $f_q + f_h = 1$ ) and defining  $\sigma$  as the given ratio of entropy to baryon densities,

$$\sigma = f_q[s_q(\mu, T)/n_q(\mu, T)] + f_h[s_h(\mu, T)/n_h(\mu, T)]. \tag{3.5}$$

Since  $f_q$ ,  $f_h$  and  $\sigma$  are chosen and  $\mu$  is known as a function of  $T$  from Eq. (3.4), Eq. (3.5) can be solved for  $T$ . The temperature and pressure will be different for different ratios of the phases. This is usually a difficult procedure even for simple equations of state. When baryons are introduced there may be pressure gradients within a region of mixed phase.

#### IV. SPHERICALLY EXPLODING PLASMA

The effects of the phase transition on the interferometry are most apparent when the initial conditions are such that the difference in pressure due to the energy being absorbed into latent heat is most manifest. We give the computer-generated solutions for three choices of initial conditions. Each case is solved for both the bag-model equation of state and for the equation of state of an ultrarelativistic pion gas without a phase transition. A plasma that is almost entirely in the mixed phase and initially static shows the most dramatic change in the dynamics when the phase transition is introduced. Here the pressure is constant in the region of mixed phase and an initially static plasma requires pressure gradients in order to accelerate radially and expand. The case where the ini-

tial energy densities are high enough that much of the matter is completely in the deconfined phase shows the same signals though not as strongly. The signals are greatly reduced for the third case where an initial radial velocity distribution is introduced.

The initial conditions were chosen to describe a large spherically symmetric fireball where all the energy is within 8 fm of the center. The initial energy density was scaled such that it would be a maximum at the center and go to zero at 8 fm:

$$\begin{aligned} \rho_0(r) &= \rho_0(1 - r^2/R^2), \quad r < R = 8 \text{ fm}, \\ \rho_0(r) &= 0, \quad r > R. \end{aligned} \quad (4.1)$$

The maximum energy density  $\rho_0$  was picked to be 2 GeV/fm<sup>3</sup> in the first and third example so that the center was in the mixed phase and nearly into the quark phase while the second example has a  $\rho_0$  of 5 GeV/fm<sup>3</sup> which corresponds to the deconfined phase. The initial velocity for the third example was chosen to increase radially from

the center:

$$\gamma v(r) = r/R. \quad (4.2)$$

The numerical technique used to solve the equations of motion are described in Appendix A. Energy and entropy are conserved explicitly. The entropy is divided into shells and followed throughout the calculation. When the outermost shell reaches the breakup temperature of 120 MeV the shell is removed from the calculation and the velocity, position, and time of the shell's breakup is stored. (At 120 MeV the mean free path of pions in a pion gas approaches the size of the system.) This information is sufficient to calculate the emission function  $g$  from which the correlation function can be determined. The technique for calculating the correlation function for a set of expanding thermal shells is shown in Appendix B.

Figure 3 shows the energy density  $T_{00}$  and the velocity  $\gamma v$  as a function of time for the case where the matter is initially static and almost entirely in the mixed phase. The matter in the mixed phase cannot move since there

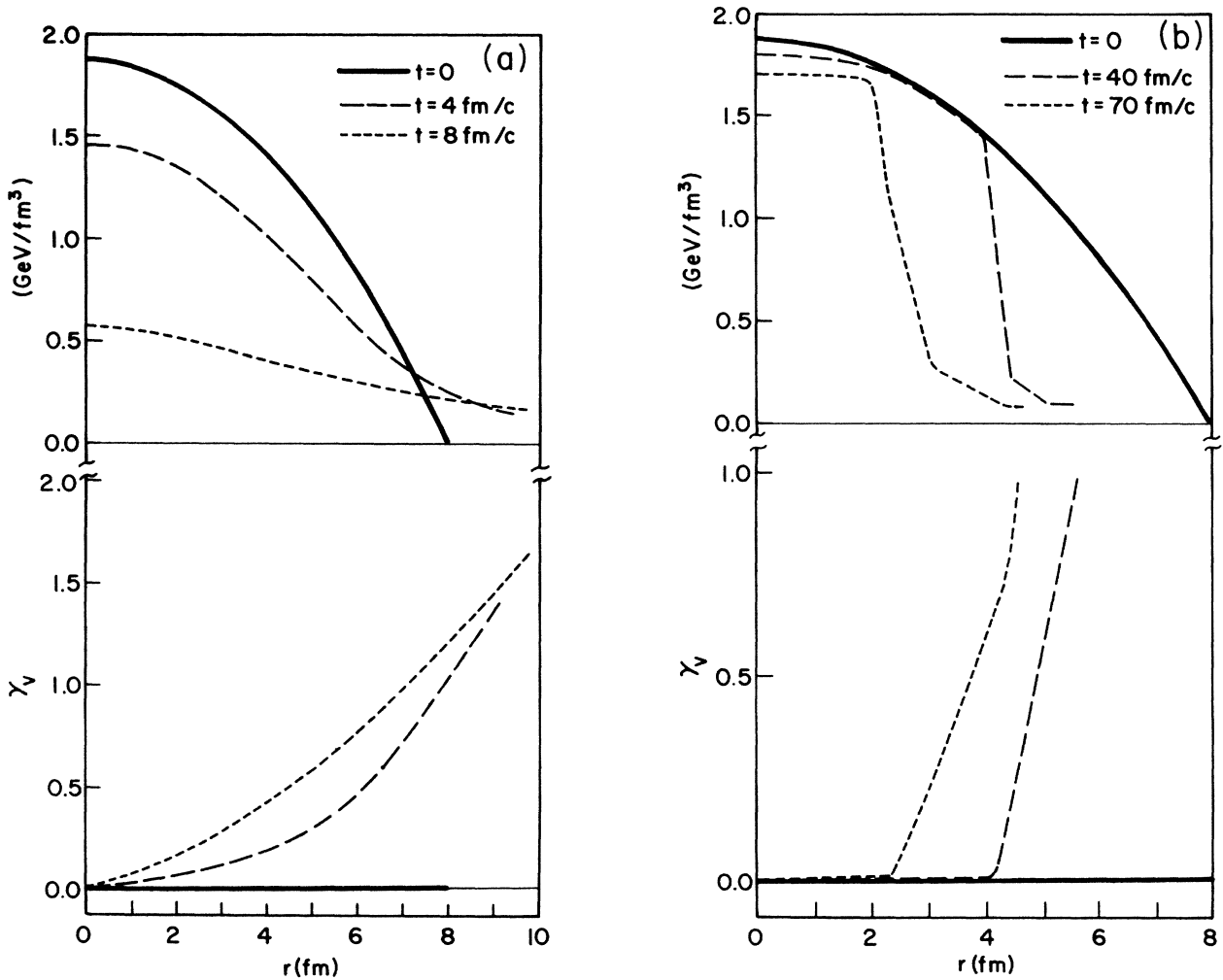


FIG. 3. (a) Initially static spherically symmetric matter described by a free gas of pions expands and dissolves in 10 fm/c. The total energy density is shown in GeV/fm<sup>3</sup>. The velocity  $\gamma v$  increases from the center and with time. (b) When a phase transition is introduced the expansion is greatly slowed so that it lasts 90 fm/c. Since the matter inside is in a mixed phase at constant pressure, a shock wave approaches from the outside.

are no pressure gradients. A shock wave approaches from the outside at a very slow velocity. Shock waves usually generate entropy but this code conserves entropy exactly. In Appendix B the characteristics of shock waves between the mixed and hadronic phases are derived for both the cases of maximum and zero entropy generation. The speed at which the shock wave advances varies only slightly when the entropy is allowed to be a maximum. The amount of entropy generated is never more than a few percent. The case of maximum entropy generation does yield noticeably higher temperatures and lower velocities immediately outside the front, but after a very short time the matter will have accelerated and cooled to look very much like the case with no entropy generated. The computer model cannot be compared to the solutions in Appendix B since the mesh size is too rough to distinguish the boundary of the front very accurately and the breakup temperature is often lower than the temperature outside the front solved for in Appendix B. However, the speed at which the front encroaches into the mixed phase does follow the solution given in the Appendix to within about ten percent. A finer mesh seems to lower the speed of the front and better approach the solutions.

The first example shows that the matter does not completely dissolve until 90 fm/c. Running the program with the hadronic equation of state yields complete dissolution in 10 fm/c. The collective or explosive velocity are much greater without the phase transition. Both these dynamical effects have very clear signatures in the correlation

function. The long lifetime yields a much larger apparent source size when the relative momentum of the pion pair is chosen to be parallel to the average momentum. This is shown in Fig. 4. Plotting the correlation function for different average momentum, and the relative momentum perpendicular to the total momentum, shows the difference in explosive velocity. Pions of greater energy appear to come from a much smaller source when there is a higher share of the energy in collective expansion. Here the width of the correlation function increases less rapidly with increasing average momentum when a phase transition is introduced. One must remember, however, that this scenario is the most extreme. When the lifetimes are extremely long one would expect leakage of pions from the inner regions to be important. Perhaps the mixed phase could be produced with beam energies low enough that the nuclei would effectively stop each other. This scenario might then be more relevant, although the equation of state would have to be parametrized for regions with nonzero baryon number.

The same calculations are shown in Figs. 5 and 6 for the case where the initial energy density  $\rho_0$  is 5 GeV/fm.<sup>3</sup> This is well into the deconfined phase. There are now pressure gradients in the center of the plasma and the explosion starts from the inside as well as the outside. The matter quickly expands into the mixed phase where it drifts at this abbreviated explosive speed until it dissolves. The phase transition extends the lifetime of the collision to 50 fm/c from 12 fm/c. The same dynamical effects

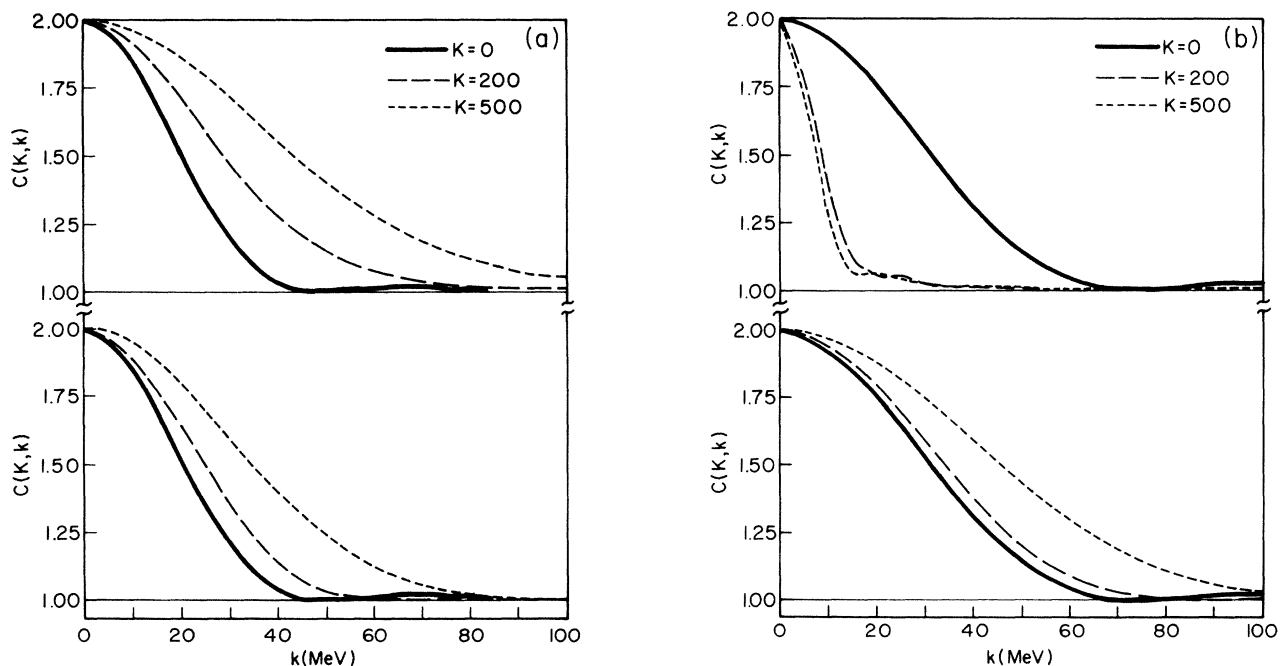


FIG. 4. (a) The correlation function is calculated from the emission function that was generated from the scenario described in Fig. 3(a). Collective expansion manifests itself through broader correlation functions for pion pairs with higher average momentum  $K$ . The upper graph shows the case where the relative momentum  $k$  is parallel to the average momentum  $K$  and the lower graph is for when the relative momentum is perpendicular to the average momentum. (b) The scenario described in Fig. 3 (b) yields these correlation functions. The phase transition brings little qualitative difference to the correlation function when the relative momentum  $k$  is perpendicular to the average momentum  $K$  (lower graph). The widths increase for pairs with higher momentum due to collective expansion. The long lifetime shows itself when  $k$  is parallel to  $K$  (upper graph). The widths then decrease for larger values of  $K$ .

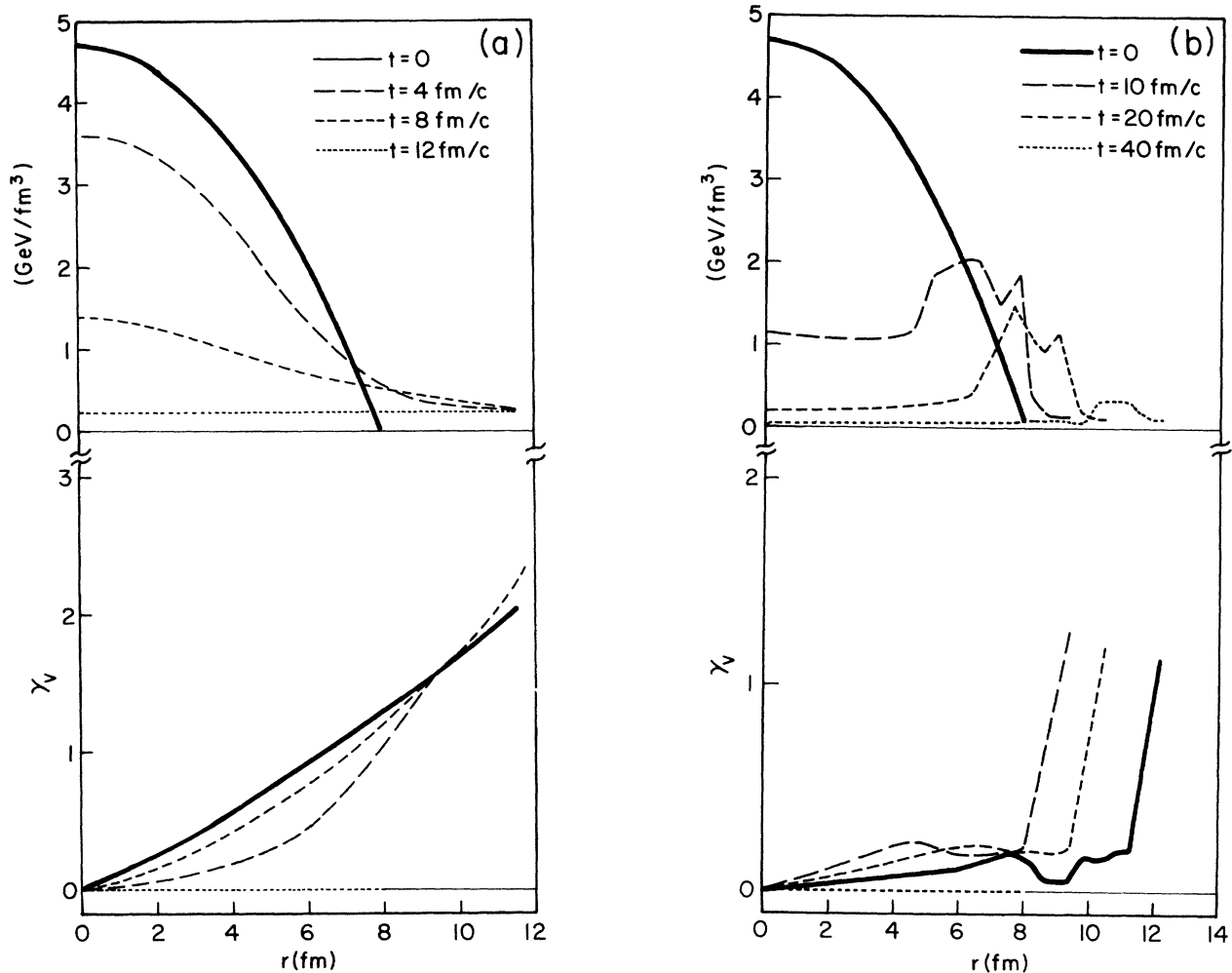


FIG. 5. (a) Here the initial energy density is higher and the matter gains more collective velocity before it explodes. The duration of the collision is longer and the outer radius is larger due to the higher initial energy density. (b) The higher initial energy density allows pressure gradients at the center since this matter is in the quark phase. The extension to the lifetime due to the transition is reduced compared to the initial conditions of Fig. 3 (a).

are signaled in the interferometry, only less dramatically than the first example. One would expect that with even higher initial energy densities the signatures would continue to fade.

The case where the initial conditions contain an initial explosive velocity is shown in Figs. 7 and 8. The lower pressures due to the phase transition manifest themselves only slightly in this scenario. The lesson to be learned here is that a strong dynamical signature for the quark gluon plasma is only expected if the plasma can be formed in a near static condition.

Until stopping power is better understood there can only be speculation as to the initial conditions of a plasma formed by heavy-ion collisions. Most of the theoretical effort in describing a quark-gluon plasma has centered on searching for signals for extremely energetic collisions, often around  $20 \text{ GeV}/\text{fm}^3$ . Here we have shown the possibility of a strong signature with a rather small energy density. If the mixed phase is produced at low bombardment energies so that the projectiles stop this calculation

becomes more realistic, although more work would be needed to include nonzero baryon number.

## V. THE BJORKEN SCALING SOLUTION

The pion spectra from ultrarelativistic hadronic collisions have been seen to be invariant to boosts parallel to the beam. This invariance extends over a substantial portion of the rapidity region in which pions are emitted. The central rapidity region is also expected to carry very few baryons which tend to stay close to the initial rapidities of the beam and target. This motivated Bjorken to find a solution to the hydrodynamic equations of motion that would retain this invariance to longitudinal boosts.<sup>10</sup> All of the hydrodynamic variables can be chosen to be a function of a proper time that is invariant to boosts along the direction parallel to the beam, the  $z$  axis:

$$\tau = (t^2 - z^2)^{1/2}. \quad (5.1)$$

The velocity and entropy density of the matter can be

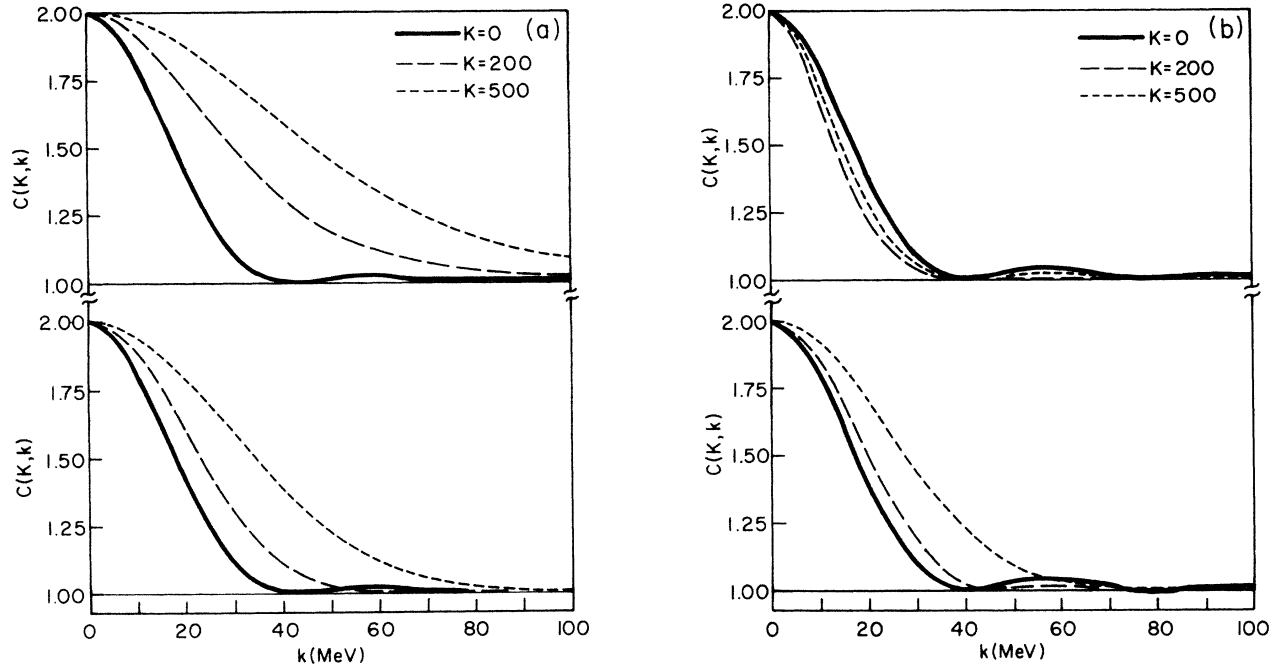


FIG. 6. (a) We show the correlation function calculated from the scenario shown in Fig. 5 (a). Collective expansion manifests itself in both cases where the relative momentum  $k$  is perpendicular (lower graph) and parallel (upper graph) to the average momentum  $K$ . Since the matter breaks up almost all at once there is little difference between the upper and lower curves. (b) Here the correlation function is shown for the case described in Fig. 5 (b). The phase transition is evidenced in the same way as the case with a lower energy density shown in Figs. 4 and 5. The extended lifetime yields a more narrow correlation function for higher momentum pairs when the relative momentum  $k$  is parallel to the average momentum  $K$  (upper graph).

written in such a way that they are independent of longitudinal boosts:

$$\gamma_z v_z = z / \tau, \quad (5.2)$$

$$s(\tau) = s(\tau_0)(\tau_0 / \tau).$$

Here  $\gamma_z$  is the Lorentz factor for the velocity  $v_z$ . The solution is considered valid only for proper times larger than some starting time  $\tau_0$ . This satisfies the hydrodynamic equations of motion for the case where no entropy is generated and the transverse degrees of freedom have been neglected:

$$\partial_\mu T^{\mu\nu} = 0, \quad (5.3)$$

$$T^{\mu\nu} = (P + \rho)U^\mu U^\nu - P g^{\mu\nu}.$$

Here  $T^{\mu\nu}$  is the stress energy tensor,  $U^\mu$  is the four velocity and  $g^{\mu\nu}$  is the metric ( $g^{00} = 1$ ). One can neglect the transverse degrees of freedom if the matter cannot expand appreciably in the transverse direction during the longitudinal lifetime of the system. This should be the case when the transverse size divided by the sound velocity is much greater than the breakup time  $\tau$ . We consider only this simple case, where the transverse dimensions are kept fixed in time, and the temperature is considered to be independent of the transverse position. A first-order phase transition would slow the transverse expansion, strengthening this assumption.

Here we solve for the correlation function due to such an expansion where the pions are all emitted at the same proper time  $\tau$  at a breakup temperature  $T$ . The correlation function does not depend on  $\tau_0$  since the emission function only depends on the properties of the matter at breakup, not at any previous time. In the center-of-mass frame the matter at  $z=0$  reaches the breakup temperature first. The matter at  $z$  breaks up at  $t = (\tau^2 + z^2)^{1/2}$ . The emission function at  $z=0$  is

$$g(\mathbf{p}, z=0, t) = \exp(-E_p/T) \delta(t - \tau). \quad (5.4)$$

Using the fact that  $E_p g(p, x)$  is a Lorentz invariant the emission function at any position  $z$  is given by

$$g(\mathbf{p}, z, t) = \exp[-\gamma_z(E_p - v_z p_z)/T] \delta(\gamma_z(t - v_z z) - \tau) \\ \times \gamma_z(E_p - v_z p_z)/E_p. \quad (5.5)$$

The correlation function should be invariant to boosts along the  $z$  axis since the emission function is invariant. Therefore the correlation function only has to be solved for when the average momentum is perpendicular to the axis.  $C(\mathbf{p}, \mathbf{q})$  can be solved for explicitly in this case:

$$C(\mathbf{p}, \mathbf{q}) = 1 + I_z I(x, y) I_z^* I^*(x, y) / [P(\mathbf{p}) P(\mathbf{q})], \quad (5.6)$$

where  $I(x, y)$  and  $I_z$  are given by

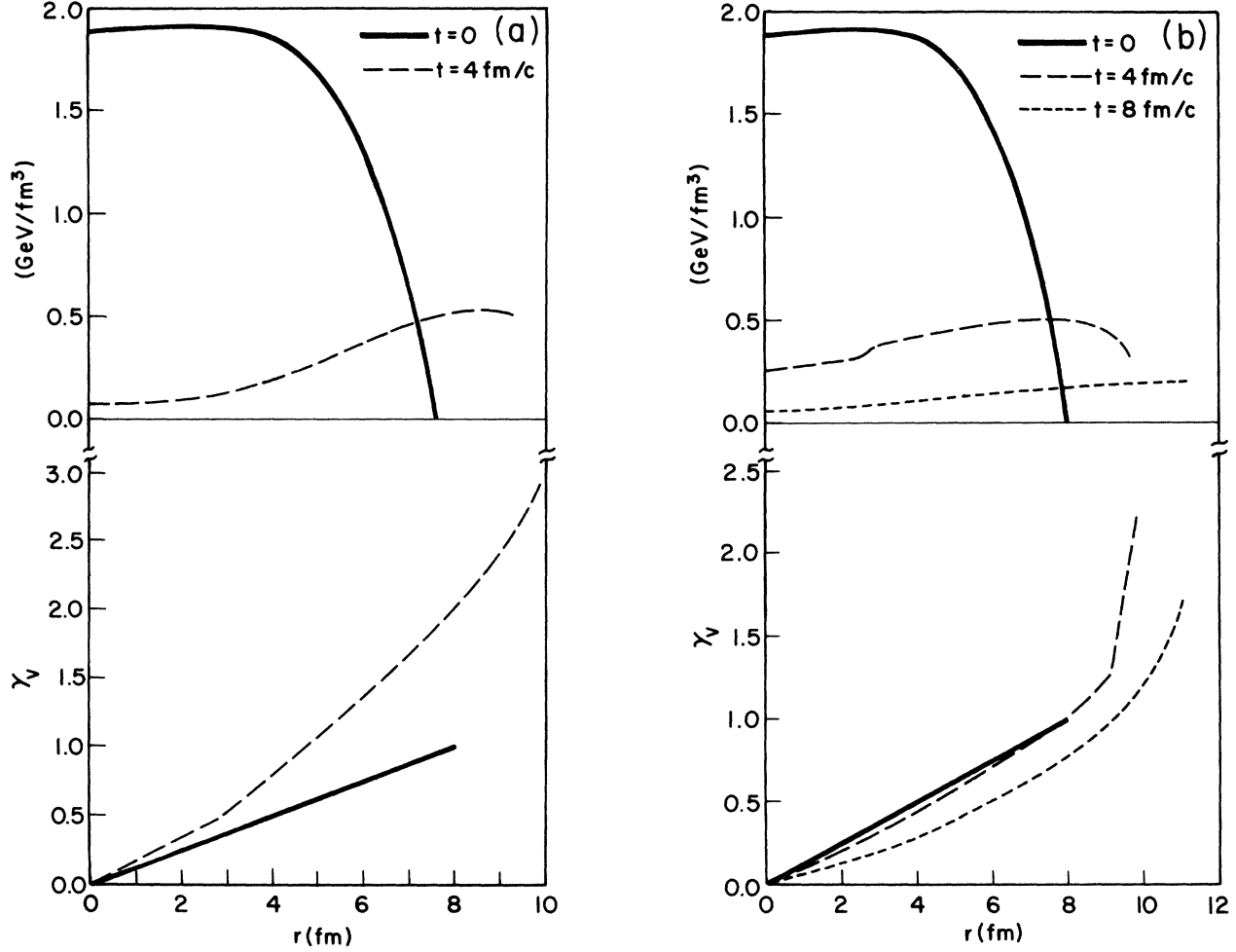


FIG. 7. (a) Here an initial explosive velocity is introduced. Pressure gradients are not needed for the matter to expand. The initial thermal energy density distribution is the same as that in Fig. 3. (b) Introducing a phase transition extends the length of the calculation from 8 to 12 fm. This is much less dramatic than the previous scenarios.

$$I(x,y) = \int_A dx dy e^{ik \cdot (x+y)},$$

$$I_z = \int dz \exp[ik_z z - ik_0(t^2 + z^2)^{1/2}]$$

$$\times \exp[-E_k(\tau^2 + z^2)^{1/2}/T\tau].$$

The single-particle probabilities  $P(\mathbf{p})$  are related to the probability of emitting a particle with zero longitudinal momentum and the same transverse momentum  $p_t$ :

$$P(\mathbf{p}) = P(p_t)(1 - p_z^2/p_0^2)^{1/2}, \quad (5.7)$$

$$P(p_t) = \int_A dx dy \int dz \exp[-E_{p_t}(\tau^2 + z^2)^{1/2}/T\tau].$$

The correlation function can be found explicitly for the case that  $k$  is along the  $z$  axis. The answer is a function of  $k_z\tau$  and the energies are measured in units of the temperature:

$$C(\mathbf{p}, \mathbf{q}) = 1 + (\beta_p \beta_q) K_1^2(\beta_k^2 + k_z^2 \tau^2)$$

$$\times [K_1^2(\beta_k)(\beta_k^2 + k_z^2 \tau^2)]^{-1}, \quad (5.8)$$

where  $\beta_p = E_p/T$  and  $K_1$  is the first-order Bessel func-

tion. If the temperature is known the lifetime  $\tau$  can be extracted from the width of the correlation function. Plotting the correlation function for different total momenta would give a good measure of the temperature. In Fig. 9 the correlation function is plotted for several values of the total energy when  $T = 120$  MeV and  $\tau = 5$  fm/c.

A phase transition could make a difference in the proper time at breakup. For a given initial energy density and  $\tau_0$  the plasma or mixed phase allows a higher initial entropy than a pure pion phase. Assuming that entropy is conserved, and that the breakup criteria only depend on the final entropy density, this allows a longer breakup time. The time is lengthened by the ratio of the initial entropy densities. For high initial energy densities the initial entropy is larger by a factor of  $(37/3)^{1/4}$ . Measuring the initial conditions is very difficult and almost by definition cannot be done with interferometry since the correlation function depends only on the final emission function. Viewing the initial conditions could only be done by viewing more exotic particles which might escape unscathed from the primary stages of the collision.

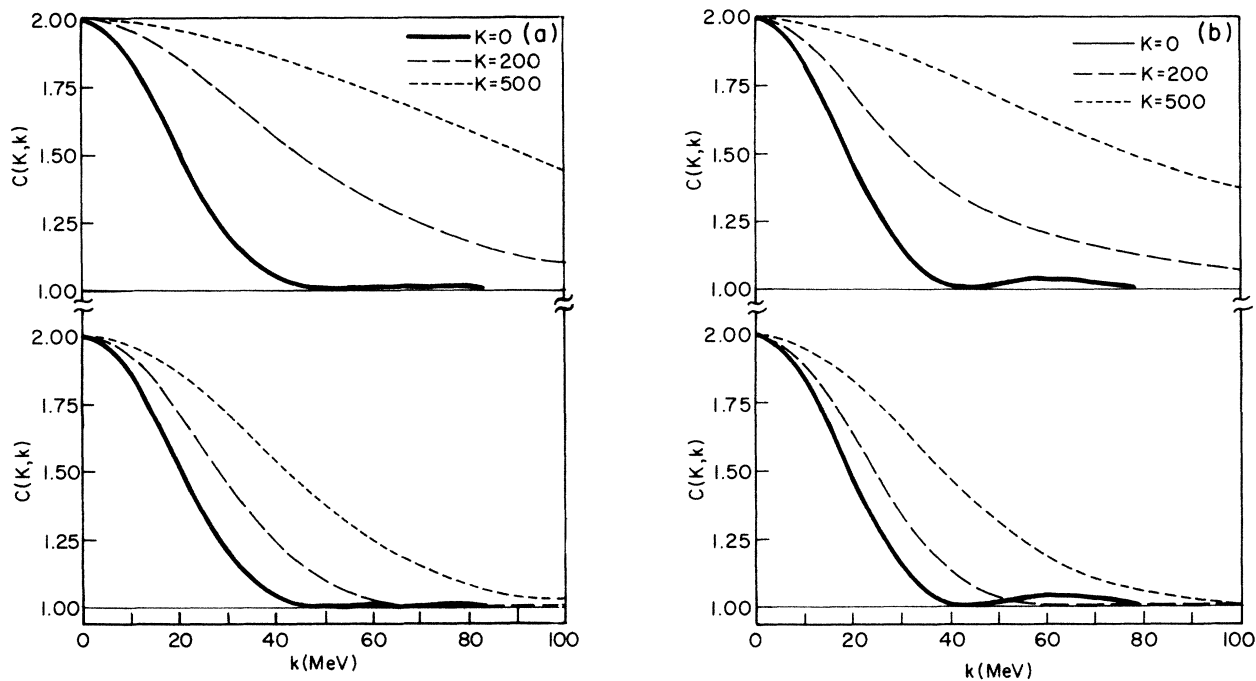


FIG. 8. (a) The correlation function is calculated from the case described in Fig. 7 (a). There is little difference between these correlation functions and those shown in Fig. 4 (a). The relative momenta  $k$  are shown perpendicular (lower graph) and parallel (upper graph) to the average momentum  $K$ . (b) The introduction of the phase transition brings little difference to the lifetime of the collision since the expansion is dominated by the initial explosion. The only marginal difference between the correlation functions is when the relative momentum  $k$  is plotted perpendicular (lower graph) rather than parallel (upper graph) to the total momentum  $K$ .

## VI. CONCLUSIONS

Pion interferometry can nearly determine the emission function. Although the correlation function  $C(p_x, p_y, p_z; q_x, q_y, q_z)$  depends on six independent variables and the emission function  $g(p_x, p_y, p_z; x, y, z, t)$  depends on seven, the correlation function contains a wealth of information. If the emission function is known to obey some constraints such as thermal emission and spherical symmetry then the correlation function should in principle

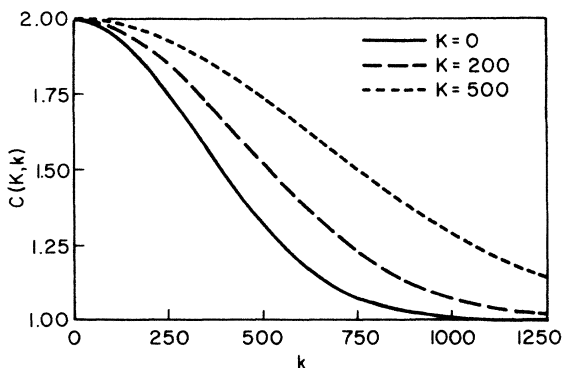


FIG. 9. The correlation function due to a Bjorken expansion is shown for the total momentum  $K$  being perpendicular to the beam and the relative momentum  $k$  being parallel. All the matter dissolves at the same proper time  $\tau$ . The width increases with larger values of  $K$ . This is a way of viewing the breakup time  $\tau$ .

uniquely describe an emission function. Although it is not feasible to measure the correlation function for all combinations of momenta, an experiment can yield good insight into the lifetime and the explosive velocity by measuring the width of the correlation function for different directions of the relative momentum and different magnitudes of the total momentum.

The emission function can give strong hints as to the properties of the system at earlier times as well. Investigation of spherical sources shows that an anomalously long-lived source with a smaller explosive velocity is a signal of a first-order phase transition with a large latent heat. This dependence is especially striking when the initial energy density was close to that of the critical energy density for entering the quark-gluon phase entirely. Another explanation for a long-lived source could be large viscosities which slow the expansion. This scenario would necessitate a growing source, which would mean a larger source size and a very low explosive velocity.

Unless the matter is initially static there probably is not such an extraordinary signal to the equation of state as the one mentioned above. However, the size, lifetime, and explosive velocity of the source are always important tests of any picture of the collision. Any model of the collision such as hydrodynamics or intranuclear cascade, will predict an emission function and therefore a unique correlation function. For instance, the solution to Bjorken's model shows a very clear structure in its dependence on the total momentum of the pion pair and its invariance to boosts. Combining the interferometric information with that from single-particle emission spectra and the mea-

surement of exotic species should give good insight into the properties of the matter in the early stages of the collision.

If it were possible the best method to study the quark-gluon plasma would be to measure the temperature and pressure by inserting a gauge. Three extensive quantities must be measured to obtain an equation of state for a static gas with no nonzero conserved charges. In heavy-ion collisions the total energy and entropy can always be estimated from experiment. (The entropy is proportional to the pion number.) Knowing the volume and fraction of collective energy for a given time of the collision would be sufficient to yield a single value in an equation of state corresponding to the conditions at that time. The correlation function can give a good estimate of both size and explosive energy at breakup. Discerning any information about the equation of state at previous times necessitates some trust in a set of initial conditions and a scenario for the expansion. If the initial conditions could be checked by measuring the abundance of hadrons or leptons that would be produced and that escape during this early stage, then experiments could check both the beginning and end of any theoretical picture.

#### ACKNOWLEDGMENTS

This work was supported by the U.S. Department of Energy under Contract No. DOE/DE-AC02-79er-10364. The author wishes to thank Joseph Kapusta for his very generous assistance and guidance.

#### APPENDIX A: COMPUTER-GENERATED SOLUTIONS TO THE HYDRODYNAMIC EQUATIONS OF MOTION

The hydrodynamic equations of motion are solved with a code designed to conserve energy and entropy explicitly. The spherical source is divided into 80 shells with an equal amount of energy in each shell at the beginning of the calculation. The entropy for each cell is then chosen to give the appropriate energy. The positions of the cell boundaries are stored for integral multiples of the time step  $\delta t$ . The velocities are stored for integer plus one-half values of  $\delta t$ . The velocities will be specified for the center of each cell. The cell boundary denoted by  $i$  is found at a later time step from quantities at earlier time steps using the formula:

$$r_i(t + \delta t) = r_i(t) + [v_i(t + \delta t/2) + v_{i+1}(t + \delta t/2)]\delta t/2. \quad (\text{A1})$$

The subscript  $i$  for the velocity refers to the cell bounded by  $r_i$  and  $r_{i-1}$ . The velocities at a later time step are found by solving the conservation of energy condition for the velocity. The energy  $E_i(t)$  at an integral time step is a

function of the cell boundary positions  $r_i(t)$  and  $r_{i-1}(t)$ , the entropy  $S_i$  and the velocity  $[v_i(t + \delta t/2) + v_i(t - \delta t/2)]/2$ ,

$$E_i = 4\pi/3(r_i^3 - r_{i-1}^3)[\rho_i\gamma^2 + P_i(\gamma^2 - 1)]. \quad (\text{A2})$$

If the energy distribution  $E_i$  is known the only unknown is the velocity  $v_i(t + \delta t/2)$ , which can be solved for. The energy density in the rest frame  $\rho$  and the pressure  $P$  must be given in terms of the entropy density. If there was another conserved quantum number such as the baryon number, that would also be stored and like the entropy it would be conserved for each cell. The equation of state would then be a function of each conserved quantity. It is difficult to write an equation of state in terms of the entropy density and baryon density when a nonzero baryon number is introduced. With zero baryon number the pressure and energy density are proportional to  $s^{4/3}$ .

A prescription has not yet been given for finding the energies  $E_i(t)$  in terms of the quantities that are prior to  $t + \delta t/2$ . Once this is found the velocity  $v_i(t + \delta t/2)$  can be solved for using the method of the above paragraph using only quantities from previous times. The energy of a specific cell changes by doing work on its outside cell and having work done on it by the inside cell. This can be shown using the conservation-of-energy condition for the energy-momentum tensor for a system with no viscosity or heat conductivity:

$$\partial_\mu T^{\mu 0} = 0, \quad (\text{A3})$$

$$T^{\mu\nu} = (P + \rho)U^\mu U^\nu - P g^{\mu\nu}.$$

The change in energy for a cell characterized by a volume  $V$  during a small time step  $\delta t$  comes from the change in energy density inside the volume and the new energy density captured by the changing boundaries:

$$\delta E = \delta t \left[ \int d^3r \partial_0 T^{00} + \oint dA v T^{00} \right]. \quad (\text{A4})$$

The first integral can be changed to an integral over the surface by using the conservation of energy condition, Eq. (A1), to change the term to an integral of a divergence and then using the divergence theorem to obtain

$$\delta E = \delta t \left[ \oint dA n_i (-T^{0i} + v_i T^{00}) \right]. \quad (\text{A5})$$

Using the definition of  $T^{\mu\nu}$  yields the result

$$\delta E = -\delta t \oint P \mathbf{v} \cdot d\mathbf{A}. \quad (\text{A6})$$

This is the familiar result from thermodynamics when there is no viscosity or heat transfer:  $\delta E = -P dV$ .

The energy  $E_i(t)$  can now be written as a function of quantities at times no later than  $t$  ( $P_{\text{in}}$  and  $P_{\text{out}}$  refer to the average pressures at the boundaries of the shell during the time interval during which work was done):

$$\begin{aligned} E_i(t) &= E_i(t - \delta t) - \frac{4\pi}{3} \{ P_{\text{out}}[r_i^3(t) - r_i^3(t - \delta t)] + P_{\text{in}}[r_{i-1}^3(t) - r_{i-1}^3(t - \delta t)] \}, \\ P_{\text{in}} &= [P_i(t) + P_{i-1}(t) + P_i(t - \delta t) + P_{i-1}(t - \delta t)]/4, \\ P_{\text{out}} &= [P_i(t) + P_{i+1}(t) + P_i(t - \delta t) + P_{i+1}(t - \delta t)]/4. \end{aligned} \quad (\text{A7})$$

This prescription yields a solution to the equations of motion that conserve both energy and entropy explicitly. Calculating a quantity requires knowledge of the quantities a full time step before the one that is being calculated. This is a problem for the first time step since the initial conditions are given for only one time. The first set of velocities were therefore calculated with the differential equations of motion:

$$v_i(\delta t/2) = -\delta t(\partial P_i/\partial r)/(P_i + \rho_i). \quad (\text{A8})$$

The breakup criteria was chosen so that when the second outermost shell reached a chosen breakup temperature the adjacent cell outside it would lose contact and any energy in the outermost shell would be emitted as pions. This cell at the breakup temperature would no longer do any work on the cell outside it and it would henceforth become the outermost shell. This restriction, that no work can be done by the outermost shell, is only physical if there is no pressure at the outer boundary. If the pressure were arbitrarily set to zero then for an infinitesimally thin outer shell a finite amount of energy would enter from the inside while none would leave at the outside. A vacuum energy  $A$  was added to the energy density everywhere and subtracted from the pressure everywhere. It was picked such that the pressure would be zero at the breakup temperature:

$$P \rightarrow P - A, \quad (\text{A9})$$

$$\rho \rightarrow \rho + A.$$

This added vacuum energy does not affect the equations of motion inside the source. However, when a cell breaks up and the energy is dissolved into free pions the energy of the pions is  $E_i = \rho\gamma^2 + A$  since the pressure is zero at breakup. Neglecting the vacuum energy  $\rho_0 = 3P_0$  for massless pions which means that  $A = \rho/4$  at breakup. Thus the vacuum term contributes one fourth of the final thermal energy. For the cases studied here the final thermal energy was of the same magnitude as the energy in collective expansion. This vacuum energy can be considered as an unthermalized energy that does not contribute to the entropy or the dynamics. It is necessary because the system is not of infinite size; thus not all the energy contributes to the pressure  $P = (\rho - 2A)/3$  and a fraction of the energy only manifests itself when the system dissolves. This crude approach is needed since viscosity and thermal conductivity have been neglected while the system is still expected to leave the hydrodynamic regime.

#### APPENDIX B: CORRELATION FUNCTION FOR SPHERICALLY EXPANDING THERMALLY EQUILIBRATED SHELLS

Here we explain how the expression for the correlation function in terms of the emission function is calculated for the case of equilibrated spherical shells of given radii dissolving into the vacuum at given times. The correlation function can be written in terms of the integrals  $I$  and  $I^*$ :

$$\begin{aligned} C(\mathbf{K}, \mathbf{k}) &= 1 + I(\mathbf{K}, \mathbf{k})I^*(\mathbf{K}, \mathbf{k})/P(\mathbf{p})P(\mathbf{q}), \\ I(\mathbf{K}, \mathbf{k}) &= \int d^4x e^{ik \cdot x} g(\mathbf{K}, x), \\ P(\mathbf{p}) &= \int d^4x g(\mathbf{p}, x) = I(\mathbf{p}, 0). \end{aligned} \quad (\text{B1})$$

The integral over time and space can be written as a sum over the given shells:  $I(\mathbf{K}, \mathbf{k}) = \sum I_n(\mathbf{K}, \mathbf{k})$ . The integrals  $I_n$  are over the angular coordinates  $\theta$  and  $\phi$  which can be done explicitly. They are functions of the radius of the shell, the velocity of the shell, the breakup temperature, and the thickness of the shell. The shell is assumed to dissolve instantaneously in the rest frame of the expanding shell. If all the shells have the same breakup temperature, the thickness of the shell in the rest frame of the shell should be proportional to the entropy of the shell divided by  $r^2$ . The emission function  $g(\mathbf{K}, x)$  is found by using the fact that  $E_k g(\mathbf{K}, x)$  and  $dr dt$  (when boosted along  $r$ ) are Lorentz invariants:

$$\begin{aligned} d^3K^* g^*(\mathbf{K}, x) dr^* dt^* &= d^3K g(\mathbf{K}, x) dr dt, \\ g^*(\mathbf{K}, x) dr^* dt^* &= (S_n/r^2) \exp(-E^*/T), \\ d^3K^*/E_k^* &= d^3K/E_k. \end{aligned} \quad (\text{B2})$$

Here the quantities marked with an asterisk refer to the rest frame of the shell. Combining these equations we find

$$g_n(\mathbf{K}, x) dr dt = (S_n/r^2)(E_k^*/E_k) \exp(-E_k^*/T). \quad (\text{B3})$$

Thus  $I_n$  becomes

$$\begin{aligned} I_n &= S_n \int d\phi d \cos\theta e^{ik \cdot x} \gamma_n (1 - \mathbf{K} \cdot \mathbf{v}_n / E_k) \\ &\quad \times \exp[-\gamma_n (E_k - \mathbf{v}_n \cdot \mathbf{K}) / T]. \end{aligned} \quad (\text{B4})$$

The velocity  $\mathbf{v}_n$  is always along the direction of  $r$ . Picking  $\mathbf{K}$  to be along the  $z$  axis and  $k_y = 0$ ,  $I_n$  is written

$$\begin{aligned} I_n &= S_n \int d\phi d \cos\theta \exp[i(k_z R \cos\theta + k_x R \sin\theta \cos\phi - k_0 t)] \\ &\quad \times \gamma_n (1 - v_n K \cos\theta / E_k) \\ &\quad \times \exp[-\gamma_n (E_k - v_n K \cos\theta) / T]. \end{aligned} \quad (\text{B5})$$

The radius of the shell is  $R$  and the breakup time is  $t$ . The integral over  $\phi$  can be performed:

$$\begin{aligned} I_n &= s_n \int d \cos\theta \exp[i(k_z R \cos\theta - k_0 t)] \\ &\quad \times 2\pi J_0(k_x R \sin\theta) \gamma_n (1 - v_n K \cos\theta / E_k) \\ &\quad \times \exp[-\gamma_n (E_k - v_n K \cos\theta) / T]. \end{aligned} \quad (\text{B6})$$

The integral over  $\cos\theta$  can also be done explicitly using the relations:<sup>11</sup>

$$\begin{aligned} \int d \cos\theta J_0(b \sin\theta) \cos(a \cos\theta) &= 2 \sin\alpha / \alpha, \\ \int d \cos\theta J_0(b \sin\theta) \sin(a \cos\theta) \cos\theta & \\ &= -2a (\cos\alpha / \alpha^2 - \sin\alpha / \alpha^3), \end{aligned} \quad (\text{B7})$$

where  $\alpha = (a^2 + b^2)^{1/2}$ . The difficulty lies in the fact that  $\alpha$  is a complex quantity. The real and imaginary parts of  $I_n$  must be separated using angle addition formulas. The results are rather lengthy:

$$I_n = S_n 4\pi\gamma_n e^{-ik_0 t} (I^R + iI^I) \exp(-\gamma_n E_k / T),$$

$$\begin{aligned} I_R = & (\alpha\alpha^*)^{-1} [(\alpha^*)_R \sin\alpha_R \cosh\alpha_I - (\alpha^*)_I \sinh\alpha_I \cos\alpha_R] \\ & + (\alpha\alpha^*)^{-2} [-A_I(\alpha^{*2})_R \cos\alpha_R \cosh\alpha_I - A_R(\alpha^{*2})_I \cos\alpha_R \cosh\alpha_I - A_I(\alpha^{*2})_I \sin\alpha_R \sinh\alpha_I + A_R(\alpha^{*2})_I \sin\alpha_R \sinh\alpha_I] \\ & + (\alpha\alpha^*)^{-3} [A_I(\alpha^{*3})_R \sin\alpha_R \cosh\alpha_I + A_R(\alpha^{*3})_I \sin\alpha_R \cosh\alpha_I \\ & - A_I(\alpha^{*3})_I \sinh\alpha_I \cos\alpha_I \cos\alpha_R + A_R(\alpha^{*3})_R \sinh\alpha_I \cos\alpha_R], \end{aligned} \quad (\text{B8})$$

$$\begin{aligned} I_I = & (\alpha\alpha^*)^{-1} [(\alpha^*)_I \sin\alpha_R \cosh\alpha_I + (\alpha^*)_R \sinh\alpha_I \cos\alpha_R] \\ & + (\alpha\alpha^*)^{-2} [+A_R(\alpha^{*2})_R \cos\alpha_R \cosh\alpha_I - A_I(\alpha^{*2})_I \cos\alpha_R \cosh\alpha_I + A_R(\alpha^{*2})_I \sin\alpha_R \sinh\alpha_I + A_I(\alpha^{*2})_I \sin\alpha_R \sinh\alpha_I] \\ & + (\alpha\alpha^*)^{-3} [-A_R(\alpha^{*3})_R \sin\alpha_R \cosh\alpha_I + A_I(\alpha^{*3})_I \sin\alpha_R \cosh\alpha_I + A_R(\alpha^{*3})_I \sinh\alpha_I \cos\alpha_R + A_I(\alpha^{*3})_R \sinh\alpha_I \cos\alpha_R]. \end{aligned}$$

The subscripts  $R$  and  $I$  refer to the real and imaginary parts of the quantity which they index. The real and imaginary parts of  $\alpha$  are

$$\begin{aligned} \alpha_R^2 = & k^2 R^2 - y^2 + [(k^2 R^2 - y^2)^2 + (2y \cdot kR)^2]^{1/2}, \\ \alpha_I^2 = & y^2 - k^2 R^2 + [(k^2 R^2 - y^2)^2 + (2y \cdot kR)^2]^{1/2}, \end{aligned} \quad (\text{B9})$$

and  $A$  and  $y$  are defined as

$$\begin{aligned} A_R = & (T/\gamma_n E_k) y \cdot kR, \\ A_I = & (-T/\gamma_n E_k) y^2, \\ y = & \gamma_n v_n K / T. \end{aligned} \quad (\text{B10})$$

The imaginary part of  $\alpha$  is always positive and the real part of  $\alpha$  is of the opposite sign of  $k_z$ . This means that  $\alpha_R$  is always the opposite sign of  $k_0$ .

The pion correlation function was calculated previously for an expanding spherical shell, however the emission function did not correspond to a thermal distribution in the rest frame of the shell for relativistic velocities. Following the procedure outlined above the correlation function can be calculated in closed form for a single shell that dissolves instantaneously in the rest frame of the shell. For a single shell:

$$\begin{aligned} C(\mathbf{K}, \mathbf{k}) = & 1 + \exp(-2\alpha E_k / T) \{ Q^{-2} (\cos 2\alpha_R + \cosh 2\alpha_I) + AA^* Q^{-4} (\cos 2\alpha_R + \cosh 2\alpha_I) \\ & + AA^* Q^{-6} (-\cos 2\alpha_R + \cosh 2\alpha_I) + AA^* Q^{-6} (-2\alpha_R \sin 2\alpha_R - 2\alpha_I \sinh 2\alpha_I) \\ & - (2\alpha_R A_I - 2\alpha_I A_R) Q^{-4} \sin 2\alpha_R + (2\alpha_R A_R + 2\alpha_I A_I) Q^{-4} \sinh 2\alpha_I \\ & + [2(\alpha_R^2 - \alpha_I^2) A_I - 4\alpha_R \alpha_I A_R] (\cos 2\alpha_R + \cosh 2\alpha_I) \} / 2 [P(\mathbf{p})P(\mathbf{q})], \end{aligned} \quad (\text{B11})$$

where  $Q^2 = \alpha_R^2 + \alpha_I^2$ .  $P(\mathbf{p})$  is the single-particle emission probability to within a constant,

$$P(\mathbf{p}) = \exp(-\gamma E_p / T) [\sinh(y_p) / y_p + (T / \gamma E_p y_p) \sinh(y_p) - (T / \gamma E_p) \cosh(y_p)],$$

where  $E_p$  is the energy of a pion with momentum  $\mathbf{p}$  and  $y_p = \gamma v_p / T$ . This gives the correlation function in closed form for a single shell. Viewing this by itself illustrates how interferometry is affected by expansion.

### APPENDIX C: SHOCK FRONTS

Here we derive the properties of shock fronts between the mixed phase and the hadronic phase. If matter in the mixed phase is surrounded by matter in the hadronic phase it must eventually expand since it is at a higher pressure. But there are no pressure gradients inside the mixed phase and the sound velocity is zero, which means that a shock front must develop in order for the matter to

expand. This shock front is a discontinuity in the pressure, energy density, entropy density, and the velocity. We will solve for the temperature and velocity of the hadronic matter outside the front and the speed at which the front moves inward through the matter. These three unknowns should only depend on the entropy density of the matter inside the front and the amount of entropy generated by the front. Conservation of momentum and energy across the front provide two conditions, and entropy flow provides the third condition, that is necessary to solve for the three unknowns. Unlike most shocks there does exist a solution where there is no entropy generated. It is not clear how much entropy should be generated by the front. The answer should depend on microscopic properties of the matter. The maximum amount of entropy that a shock can generate is never more than a few per cent but the speed at which the shock approaches inward, and the speed of the ejected matter, could vary substantially. Here we give two solutions to the equations governing the front. The first solution corresponds to a

shock with no entropy generation. The second is the solution for maximum entropy generation. This turns out to be identical to the solution given by Baym<sup>9</sup> where the ejection velocity in the frame where the shock is at rest was chosen to be the speed of sound of the hadronic matter. This solution also turns out to be the solution that allows the shock front to move inwards at the highest speed.

Energy and momentum conservation are expressed by the Rankine-Hugoniot relations. The subscripts refer to the matter in the mixed and hadronic phases on either side of the discontinuity. In the frame where the shock front is at rest,

$$(P_m + \rho_m)\gamma_m^2 v_m^2 - (P_h + \rho_h)\gamma_h^2 v_h^2 = P_m - P_h, \quad (C1)$$

$$(P_m + \rho_m)\gamma_m^2 v_m = (P_h + \rho_h)\gamma_h^2 v_h.$$

The first equation demonstrates that the momentum flow across the front changes by the pressure difference. The second equation states that the energy flow is the same on both sides of the front. The next condition is for the entropy to be generated ( $F$  is the ratio of the new entropy to the old entropy):

$$s_h \gamma_h v_h = F s_m \gamma_m v_m. \quad (C2)$$

Using the Rankine-Hugoniot relations the velocities can be solved for in terms of the pressures and energy densities inside and outside the front:

$$\begin{aligned} \gamma_h^2 v_h^2 &= (P_h - P_m)(\rho_m + P_h) \\ &\times [(P_h + \rho_h)(\rho_h - \rho_m + P_m - P_h)]^{-1}, \end{aligned} \quad (C3)$$

$$\begin{aligned} \gamma_m^2 v_m^2 &= (P_h - P_m)(\rho_h + P_m) \\ &\times [(P_m + \rho_m)(\rho_h - \rho_m + P_m - P)]^{-1}. \end{aligned}$$

The temperature can be written in units of  $T_0$  and the pressures and energy densities can be written in units of the critical pressure. We define  $x$  as the ratio of entropy in the mixed phase to the critical entropy density at which one starts to enter the mixed phase from the pure hadronic phase. In these units:

$$\begin{aligned} P_m &= 1, \\ T_m &= 1, \\ s_m &= 4x, \\ \rho_m &= 4x - 1, \\ P_h &= T_h^4, \\ \rho_h &= 3T_h^4, \\ s_h &= 4T_h^4. \end{aligned} \quad (C4)$$

Using the fact that  $P + \rho = Ts$ , we can calculate  $F$  in terms of  $T_c$  and  $x$ :

$$F^2 = T_h^2(4x - 1 + T_h^4)/x(3T_h^4 + 1). \quad (C5)$$

For a given  $F$  this could be solved as a cubic equation for  $T_h^2$ . For  $F=1$  the cubic equation can be factored into a solution with  $T_h^2=1$  and a quadratic equation. The solu-

tion of  $T_h=1$  corresponds to nothing happening. The matter on each side of the front would not be moving. This certainly would not violate any of the conservation laws. The active solution to the quadratic equation yields:

$$T_h^2 = (3x - 1)/2 - (\frac{1}{2})[(9x - 1)(x - 1)]^{1/2}. \quad (C6)$$

The temperature is shown in Fig. 10 as a function of  $x$ , the ratio of the entropy density in the mixed phase. The temperature approaches  $3^{-1/2}T_c$  as  $x$  increases. The velocity of the ejected matter and speed of the shock are shown in Fig. 10. These are shown in the frame where the matter in the mixed phase is at rest. The ejected matter has vanishing velocity as  $x$  approaches unity, and the velocity approaches  $(2/3)^{1/4}$  as  $x$  becomes large. The shock front advances into the mixed phase at the speed of sound of the hadronic phase  $(1/3)^{1/2}$  as  $x$  approaches unity, and the front velocity goes to zero for large values of  $x$ . Thus if matter can be produced in the mixed phase with no initial expansion velocity the matter can stay in that phase much longer than it could have if it had a nonzero speed of sound.

The Rankine-Hugoniot equations and Eq. (C2) can also be solved for the case where  $F$  is maximized. This solution gives  $v_h = (1/3)^{1/2}$  for all values of  $x$ , which is the condition Baym imposed in his solution to the Rankine-Hugoniot equations. The temperature of the ejected

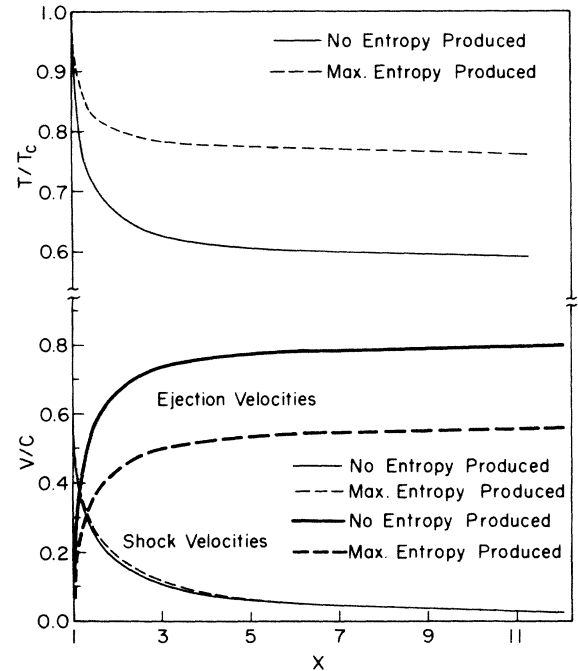


FIG. 10. The properties of a shock front are plotted against the entropy density of the matter in the mixed phase which is inside the front. The entropy is shown in units of the critical entropy necessary to enter the mixed phase. We show the temperature of the hadronic matter ejected from the shock, the velocity of the ejected hadronic matter, and the velocity that the shock front moves inward. These velocities are measured in the frame of the matter in the mixed phase. Solutions are shown for the case of no entropy generation and for the case of maximum entropy generation.

matter is higher than when there is no entropy generation as shown in Fig. 10:

$$T_h^4 = 2x - 1 - 2[(x-1)(x-1/3)]^{1/2}. \quad (C7)$$

The velocity of the front is also maximized with this solution. But it varies very little from the case where no entropy is generated. This is probably the physical solution to the equations. Since a shock front is a discontinuity there is no reason to expect entropy to be conserved. Entropy is conserved only when the mean free path is much shorter than a characteristic length over which the system changes. The amount of entropy that can be generated for a given value of  $x$  is shown in Fig. 11.

There are two solutions to the Rankine-Hugoniot equations for any given value of  $F$  lower than the one for maximizing  $F$ . One set of solutions lies between the solutions for no entropy generation and maximum entropy generation. In the frame of the shock these solutions all have the velocity of the ejected matter greater than the sound velocity. These solutions are probably unphysical since the ejected matter loses contact with the front. The other set of solutions lies between that for maximum entropy generation and the trivial solution for no entropy generation where all the velocities are zero. In the frame of the shock the ejection velocities are all less than the speed of sound.

It is not clear what should govern the choice of solutions. If nucleation rates do not provide microscopic con-

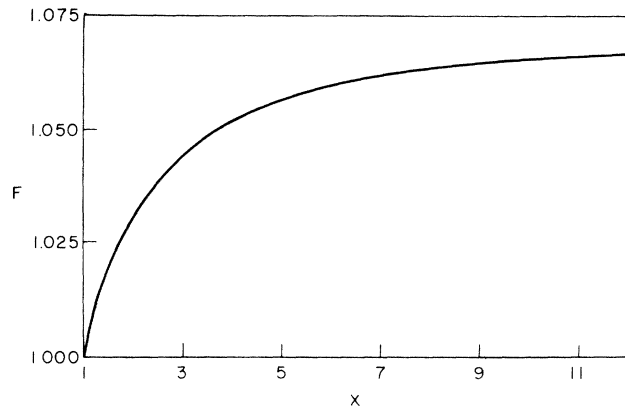


FIG. 11. The maximum allowed entropy production is plotted against the entropy density of the mixed phase. The entropy generation is never more than 7.5%.

straints on the speed at which the front advances into the mixed phase, then the solution should be the one that produces the most entropy. Without a microscopic model of the plasma this cannot be determined. However, if the solution were one besides that for maximum entropy generation, the front would advance even slower and the effects of the phase transition on the dynamics and the interferometry would be even greater than those reported here.

<sup>1</sup>J. Rafelski and B. Muller, Phys. Rev. Lett. **48**, 1066 (1982).

<sup>2</sup>L. McLerran and T. Toimela, Phys. Rev. D **31**, 545 (1985).

<sup>3</sup>M. Gyulassy, K. Kajantie, and L. McLerran, Nucl. Phys. **B237**, 477 (1984).

<sup>4</sup>G. I. Kopylov, Phys. Lett. **50B**, 472 (1974).

<sup>5</sup>S. Pratt, Phys. Rev. Lett. **53**, 1219 (1984).

<sup>6</sup>M. Gyulassy, S. K. Kauffmann, and Lance Wilson, Phys. Rev. **C 20**, 2267 (1979); S. Pratt (unpublished).

<sup>7</sup>T. Celik, J. Engels, and H. Satz, Nucl. Phys. **B205**, 545 (1983).

<sup>8</sup>J. Kapusta, D. Reiss, and S. Rudaz, University of Minnesota Report No. DOE/ER/40105-513, 1984 (unpublished).

<sup>9</sup>G. Baym *et al.*, Nucl. Phys. **A407**, 541 (1983).

<sup>10</sup>J. D. Bjorken, Phys. Rev. D **27**, 140 (1983).

<sup>11</sup>I. S. Gradshteyn and I. M. Ryzhik, *Table of Integrals, Series and Products* (Academic, New York, 1980).